

RSC Advances



This is an *Accepted Manuscript*, which has been through the Royal Society of Chemistry peer review process and has been accepted for publication.

Accepted Manuscripts are published online shortly after acceptance, before technical editing, formatting and proof reading. Using this free service, authors can make their results available to the community, in citable form, before we publish the edited article. This *Accepted Manuscript* will be replaced by the edited, formatted and paginated article as soon as this is available.

You can find more information about *Accepted Manuscripts* in the [Information for Authors](#).

Please note that technical editing may introduce minor changes to the text and/or graphics, which may alter content. The journal's standard [Terms & Conditions](#) and the [Ethical guidelines](#) still apply. In no event shall the Royal Society of Chemistry be held responsible for any errors or omissions in this *Accepted Manuscript* or any consequences arising from the use of any information it contains.

Preparation of ROMP-type Imidazolium-Functionalized Norbornene Ionic Liquid
Block Copolymer and Electrochemical Property for Lithium-ion Battery
Polyelectrolyte Membranes

Juan Wang¹, Xiaohui He^{1,2*}, Hongyu Zhu¹, and Defu Chen³

¹School of Materials Science and Engineering, Nanchang University, 999 Xuefu
Avenue, Nanchang 330031, China

²Jiangxi Provincial Key Laboratory of New Energy Chemistry, Nanchang University,
999 Xuefu Avenue, Nanchang 330031, China

³School of Civil Engineering and Architecture, Nanchang University, 999 Xuefu
Avenue, Nanchang 330031, China

ABSTRACT: Imidazolium-functionalized norbornene ionic liquid block copolymers are synthesized via ring-opening metathesis polymerization (ROMP). The solid polyelectrolytes were prepared by blending the copolymers with various contents of lithium bis(trifluoromethanesulphonyl)imide. The effects of polymerized ionic liquids (PILs) compositions on the properties, morphology, and ionic conductivity of the polyelectrolytes are investigated. The polymer with 50.7 mol% PIL displays a long-range ordered lamellar structure, and its corresponding polyelectrolyte achieves the best ionic conductivity with 7.44×10^{-6} S cm⁻¹ at 30 °C and 4.68×10^{-4} S cm⁻¹ at 100 °C, respectively. The ionic conductivity is enhanced 1 order of magnitude compared to the polyelectrolytes with lower polymerized ionic liquids block compositions. In addition, the polyelectrolytes are electrochemically stability up to 4.2 V versus Li/Li⁺, indicating their suitable electrochemical property for Lithium-ion battery application.

Keywords: block copolymers; polymerized ionic liquids; solid polyelectrolyte; lamellar structure; ionic conductivity; electrochemical property; Lithium-ion battery

* Correspondence to: Xiaohui He, School of Materials Science and Engineering, Nanchang University, Nanchang 330031, China. Email: hexiaohui@ncu.edu.cn (X. He)

1. Introduction

Solid polymer electrolytes (SPEs) have been extensively studied for several decades as an alternative for the traditional liquid electrolyte in lithium-ion batteries due to the superiority in safety and mechanical properties^[1-4]. However, the SPEs exhibit fairly low ionic conductivity at room temperature, well below the 10^{-3} S cm⁻¹ minimum required for practical batteries electrolytes^[5], and thus limits their feasibility for commercial application. So the key challenge is to improve the ionic conductivity of the solid polymer electrolytes.

Polymerized ionic liquids (PILs) display the outstanding performance of ionic liquids such as the unique nonvolatile, non-flammability, large electrochemical window, high ionic conductivity, and the good film-forming of polymers^[6-8], and thus they have been considered as a new type of materials of solid polymer electrolytes. Recently, various PIL electrolytes have been synthesized, such as tetraalkylammonium-type poly(IL)s^[9,10], imidazolium-based poly(IL)s^[11-16], and poly(pyrrolidinium)^[6,17], and the corresponding physical and chemical properties, ionic conductivity, and microphase separation have also been characterized. For example, Elabd et al.^[11,12] synthesized a series of PIL diblock copolymers, and the ionic conductivity is 0.88 mS cm⁻¹ at 25 °C. With the similar PIL compositions, the ionic conductivity of the block copolymers increased 2 orders of magnitude compared to the random copolymers, and the block copolymers film can form strong microphase-separated to further increase ionic conductivity. Moreover, Yang^[18] synthesized a novel polymeric ionic liquid owning the well thermal and electrochemical stability and high lithium ion conductivity simultaneously. Thus, the PIL electrolytes have been already applied to lithium ion battery^[9,10,13,19].

In this work, a series of imidazolium-functionalized norbornene ionic liquid block copolymers were synthesized via ring-opening metathesis polymerization (ROMP) (**Scheme 1**). We expect that the block copolymers can achieve excellent film-forming properties from the polynorbornene backbone and high ionic conductivity from a

long-range ordered imidazolium phase. The thermal properties, morphology and ionic conductivity of the block copolymer electrolytes are investigated as a function of ionic liquid block copolymers and lithium salt contents.

2. Experimental section

2.1. Materials

6-Bromo-1-hexanol, 1-Methylimidazole, Ethyl vinyl ether, 5-Norbornene-2-carboxylic acid (NBCOOH, 98%, mixture of endo and exo isomers), 4-Dimethylaminopyridine (DMAP), Lithium bis(trifluoromethanesulphonyl)imide (LiTFSI), Grubbs' catalyst first generation ($\text{Cl}_2(\text{PCy}_3)_2\text{Ru}=\text{CH-Ph}$), 1-(3-Dimethylaminopropyl)-3-ethylcarbodiimide hydrochloride (EDCI) are used as received from Energy Chemical, methyl-5-Norbornene-2-carboxylate (NBCOOCH₃) is purified by distillation over CaH₂ at a reduced pressure under a dry nitrogen purge just before used.

2.2. Synthesis of 5-norbornene-2-carboxylate-6-bromohexane (NBr)(1).

The synthesis of monomer is shown in **Scheme 1(A)**

In a 100 mL round-bottomed flask equipped with a magnetic stir bar, the EDCI (8.05 g, 0.042 mol) and DMAP (catalytic amount) are added to the 30 mL CH₂Cl₂ solution of the dissolved 5-Norbornene-2-carboxylic acid (4.7 g, 0.034 mol) and 6-Bromo-1-hexanol (5 g, 0.028 mol). Stirring the mixture at room temperature for 5 h, then the reaction is quenched by adding water (30 mL). The crude product is extracted three times with CH₂Cl₂ and the organic layer is dried with anhydrous MgSO₄. Filtered, and concentrated by rotary evaporator to afford oil product. The crude mixture is further purified by column chromatography on silica gel by using hexanes/EtOAc (20:1) to yield a yellow oil (7.2 g, 85%). ¹H NMR (400 MHz, CDCl₃): δ =6.15-5.90 (m, 2H), 4.05 (t, 2H), 3.50(m, 1H), 3.36 (t, 2H), 3.16 (s, 1H), 2.99 (s, 1H), 2.85(m, 1H), 2.13-2.22 (m, 2H), 1.92-1.79 (m, 2H), 1.68-1.21 (m, 7H).

2.3. Synthesis of 5-norbornene-2-carboxylate-1-hexyl-3-methyl-imidazolium bis((trifluoromethyl)sulfonyl)amide (NIm-TFSI) (**2**)

Compound **1** (6.5 g, 0.022 mol) and 1-Methylimidazole (2.6 mL, 0.033 mol) are refluxing in acetonitrile for 18 h. After cooling to room temperature, the reaction mixture is concentrated under reduced pressure to afford yellow viscous oil and then washed with Et₂O (3 × 100 mL). The resulting oil is dissolved in H₂O (100 mL), LiTFSI (6.53 g, 0.023 mol) is added, and the mixture is stirred at room temperature for 12 h. The yellow oil is extracted with dichloromethane and the organic layer is washed with water and dried over anhydrous MgSO₄. Monomer **2** is obtained as yellow oil (10.08 g, 80%). ¹H NMR (400 MHz, CDCl₃): δ=8.77(s, 1H), 7.30(d, 2H), 6.17-5.88(m, 2H), 4.17(t, 2H), 4.05(t, 2H), 3.98(m, 1H), 3.94(s, 3H), 3.16 (s, 1H), 2.99 (s, 1H), 2.85(m, 1H), 2.13-2.22 (m, 2H), 1.92-1.79 (m, 2H), 1.68-1.21 (m, 7H).

2.4. Synthesis of homopolymer of methyl-5-norbornene-2-carboxylate (NB-COOCH₃) (PMN)(**4**)

The synthesis of homopolymer is shown in **Scheme 1(B)**

All polymerizations are performed under a nitrogen atmosphere, tetrahydrofuran (THF) is distilled from sodium prior to using. Grubbs' catalyst first generation [Cl₂(PCy₃)₂Ru=CH-Ph] (67.0 mg, 0.08 mmol) is dissolved in 10 mL THF first, NBCOOCH₃ (0.609g, 4 mmol) is added to the solution by syringe under stirring. The reaction mixture is stirred at 30 °C, after 5 h, the reaction is terminated by ethyl vinyl ether (equivalent) and continue to stir for 1h. Then the polymer solution is precipitated in hexanes, purified, and dried under vacuum to get the brown solid.

2.5. Synthesis of ionic liquid block copolymers of methyl-5-norbornene-2-carboxylate -block- 5-norbornene-2-carboxylate-1-hexyl-3-methyl-imidazolium bis((trifluoromethyl)sulfonyl)amide (**5-9**)

The synthesis of ionic liquid block copolymers is shown in **Scheme 1(C)** and the

typical polymerization reaction is as follows. Grubbs' catalyst (167.40 mg, 0.2 mmol) is dissolved in 10 mL THF, and then NBCOOCH₃ (1.272 g, 8 mmol) is added to the solution by syringe under stirring. The reaction mixture is stirred at 30 °C, and the NBCOOCH₃ reacted completely after 5 h, which detected by ¹H NMR; the monomer **2** (1.167 g, 2 mmol) is added and continue stirring for 24 h, the reaction is then terminated by ethyl vinyl ether (equivalent) and continue stirring 1h. The polymer solution is precipitated in hexanes ^[20-22], purified, and dried under vacuum to get the brown solid (1.995 g, 84%). Similar chemical shifts are observed for polymers **5-9**.

2.6. Preparation of polyelectrolyte membranes

The polyelectrolyte membranes are prepared by separately dissolving the block copolymers and lithium salt (LiTFSI) in THF for 12 h, and the mixed compositions are in four different proportions (**Table 1**). Then the solutions are casted on PTFE molds to prepare the polyelectrolyte films. The films are dried in the nitrogen atmosphere at room temperature for 24 h, and subsequently dried under vacuum for 48 h at 40 °C. The photograph of polyelectrolyte membrane is illustrated in **Fig. 1**. The films were about 150 μm thickness (**Table 1**).

2.7. Measurements

¹H NMR spectra are recorded in deuterated solvents on a Bruker ADVANCE 400 NMR Spectrometer. ¹H NMR chemical shifts are reported in ppm downfield from tetramethylsilane (TMS) reference using the residual protonated solvent as an internal standard. Molecular weights of the PIL block copolymers are determined by using a Waters 2410 gel permeation chromatograph (GPC) with a refractive index detector in tetrahydrofuran (THF) and using a calibration curve of polystyrene standards. Thermo gravimetric analysis (TGA) is performed on a TA-600 for thermal analysis at a heating rate of 20 °C min⁻¹ under nitrogen with a sample weight of 4-10 mg. The differential scanning calorimeter (DSC, Perkin-Elmer DSC 7) is measured to determine the glass transition temperatures (T_g) of copolymers at a heating/cooling

rate of 10 °C min⁻¹. The X-ray diffraction (XRD) study of the samples is carried out on a Bruker D8 Focus X-ray diffractometer operating at 30 kV and 20 mA with a copper target ($\lambda = 1.54 \text{ \AA}$) and at a scanning rate of 1° min⁻¹. The microphase separation studying is carried on JEOL JEM-2100F transmission electron microscope (TEM). The samples are coated on Cu grids and stained by exposing to the vapor of a 5 wt % aqueous solution of RuO₄ for 2 h to enhance contrast degree between phases before testing [23]. The ionic conductivities of polymer electrolyte membranes are performed on electrochemical impedance spectroscopy (EIS) over a frequency range of 100–1 MHz with the amplitude of 10 mV at the temperature range from 30 to 100 °C. The ionic conductivity (σ) is calculated from the following equation (Eq.1):

$$\sigma = L/R \cdot S \quad (\text{Eq. 1})$$

Where the R represents the bulk electrolyte resistance, L means the sample thickness, and S is the area of the polymer electrolyte film.

3. Results and discussion

3.1. Characterization of the monomer and polymers

The chemical structure of 5-norbornene-2-carboxylate-1-hexyl-3-methyl-imidazolium bis((trifluoromethyl)sulfonyl)amide (NIm-TFSI), Poly(methyl-5-norbornene-2-carboxylate) (PMN), and PIL diblock copolymers are confirmed by ¹H NMR spectra shown in **Fig. 2**. For the imidazolium-functionalized norbornene monomer, the characteristic protons absorption peaks of double bond in norbornene ring appear at 6.12 and 5.88 ppm (**Fig. 2(a)**). But the absorption peaks transfer to 5.50-5.13 ppm after the monomer polymerization (**Fig. 2(b)**). Proton absorption peaks of imidazolium ring in the monomer and ionic liquid block copolymers appear around 8.70 (CH), 7.26 to 7.33(CH=CH) and 3.92 (CH₃) are similarly. The NBCOOCH₃ homopolymer has no protons absorption peak between 7.26 to 8.70 ppm. And as the ionic liquid block compositions increase, the proton

absorption peak areas increase gradually. The successful synthesis of the monomer and copolymers were well confirmed by the ^1H NMR spectra. The M_n of the copolymers obtained by GPC and Polymerized Ionic Liquids (PILs) block molar percentages are calculated ^[24] by ^1H NMR analysis. The related images are presented in the supporting information (**Fig. S1-S6**) and the corresponding results are exhibited in **Table 2**.

3.2. Thermal Properties

The thermal properties of copolymers are investigated by thermogravimetry analysis (TGA) and differential scanning calorimetry (DSC). All block copolymers exhibit good thermal stability with decompositions temperatures (5% weight loss) over 390 °C (**Fig. 3**), which is more stable than that of the homopolymer. (**Table 2**) The differential scanning calorimeter (DSC) curves are displayed in **Fig. 4(a)**. All the samples are heated to 250 °C to remove thermal history first. Homopolymer has only one distinct glass transition and the PIL block copolymers have two glass transitions that belong to the different blocks, these results indicate that the block copolymers have strong microphase-separated ^[11]. With the content of PIL block increases, the intensity of T_{g1} decreases, while the intensity of the T_{g2} shows the opposite tendency. Moreover, the T_g s decreases after blending with lithium salt because the large anions TFSI⁻ has weaker association with cation ^[25], and incremental content of lithium salt will further reduce the T_g s. (**Fig. 4(b)**)

3.3. Morphology of the copolymers

The microstructure of the copolymers is studied by X-ray diffraction (XRD) (**Fig. 5**). All the pure copolymer films casting from their THF solutions displayed two weak diffraction peaks in the angles of $\sim 5.6^\circ$ and $\sim 21.8^\circ$. The first reflection peak at $2\theta = 21.8^\circ$ is the fundamental building of copolymer backbone, and the broad peaks indicate the copolymers exhibiting the amorphous structure ^[26]. It remains unchanged profile when the ratio of PIL composition is varied. However, the intensity of peak at

$2\theta = 5.6^\circ$ increases along with the enhanced content of the PIL part, suggesting a more regular packing of side chain [27,28]. Transmission electron microscopy (TEM) was performed to further study the copolymers micro-morphology. The TEM images of copolymers are present in **Fig. 6**. The copolymers with 21.3 mol% PIL and 31.0 mol% PIL show some degree of microphase-separated morphology, but they have no long-range periodic order. While the 50.7 mol% PIL copolymer exhibits good lamella morphology with long-range periodic order clearly, this may be due to the difference electron densities between polynorbornene main chain and PIL side chains [29]. These microphase-separated morphologies are expected to provide a good passage for Li^+ transporting in the membranes.

3.4. Ionic Conductivity

As the homopolymer is brittle and can not form film independent, all ionic conductivities are obtained from PIL block copolymers electrolyte membranes. **Fig. 7** exhibits the temperature dependence of ionic conductivity of polyelectrolyte with different PIL ratio ranging from ca. 21.3 to 50.7 mol% with 5% LiTFSI. Obviously, the ionic conductivity increases with the rise of temperature and PIL molar ratios. This trend may be due to the stronger segmental motion caused by high temperature, which is beneficial for ionic transport [30,31]. Besides, the PIL as the ion transporters plays an important role in improving ionic conductivity. The results show that the ionic conductivity of the polyelectrolyte with 38.7 mol% and 50.7 mol% PIL increase ca. 1 order of magnitude compared to the polyelectrolyte with lower PIL compositions. **Fig. 8** reveals the ionic conductivity of 50.7 mol% PIL with different LiTFSI contents. The increasement of LiTFSI content can raise the concentration of Li ions, and result in enhancing the ionic conductivity. On the other hand, the block copolymer with 50.7 mol% PIL compositions exhibits good lamella morphology and it will provide a fixed ion transport channels [32] and help Li ions to transport easier and faster. The polyelectrolyte containing 50.7 mol% PIL and 20% LiTFSI offers the best ionic conductivity with $7.44 \times 10^{-6} \text{ S cm}^{-1}$ at 30 °C and $4.68 \times 10^{-4} \text{ S cm}^{-1}$ at 100 °C,

respectively. However, the room conductivity achieved in our study is lower compared with the literature reported homo-PIL, and it is agree with the results that the conductivity value of solid polymer electrolytes is lower than that of polymer gel electrolytes [9,10,13,33,34]. On the other side, like the other similarity PIL block copolymers [11, 12, 35], these copolymers do not apply to lithium ion battery.

The ionic conductivities of other copolymer electrolytes with different lithium salt contents are also measured (**Table 3**). As expected, the ionic conductivities increase with the enhancement of PIL compositions and LiTFSI contents.

Because the cation is fixed on the polymer chain and only the anion is mobile, PIL block copolymer electrolyte is single-ion conductor. Therefore, the connectivity of conducting (i.e., ions ion-to-ion hopping distance) has significant impact on ion transport [11]. In the PIL block units, the high concentration of ion conductors is helpful for shorting the anion-to-anion hopping distance, and leading to low hopping energy and the efficiency of ion transport. Consequently, the increased PIL compositions made the local concentration of conducting ions up-shift and thus enhanced the ionic conductivity.

From Fig.7 and Fig.8, It can be found that the ionic conductivity approximately linear increases with the temperature increasing, which obeys the Arrhenius equation (Eq.2):

$$\sigma(T) = A \cdot \exp\left(\frac{-E_a}{RT}\right) \quad (\text{Eq. 2})$$

Where σ is the ionic conductivity, A is the pre-exponential factor, E_a is the activation energy of ion conduction, and R is the gas constant and T is the absolute temperature. E_a is calculated from the slope of the fitting lines with the temperature range of 373 -303 K. The calculated E_a values are 27.56 kJ mol⁻¹ (50.7 mol% PIL/ 5% LiTFSI polyelectrolyte membrane), 26.77 kJ mol⁻¹ (50.7 mol% PIL/ 10% LiTFSI polyelectrolyte membrane), 24.78 kJ mol⁻¹ (50.7 mol% PIL/ 15% LiTFSI

polyelectrolyte membrane) and $24.39 \text{ kJ mol}^{-1}$ (50.7 mol% PIL/ 20% LiTFSI polyelectrolyte membrane), respectively. The E_a values of polyelectrolyte membranes have a small change, and it agrees with that the lower activation energy getting the higher ionic conductivity^[36].

3.5. Electrochemical stability

Electrochemical stability window of the polyelectrolyte is characterized by linear sweep voltammetry using the cell SS| polymer electrolyte |Li. In the measurement, we choose two typicality high ionic conductivity polyelectrolytes, and the results are shown in **Fig. 9**. Both of polyelectrolytes exhibit suitable electrochemical stability. Although the polyelectrolyte with PIL ratio of 31.0 mol% is relatively more stable due to the less content of ionic liquids. The polyelectrolyte of 50.7 mol% PIL compositions decomposed at about 4.2 V versus Li/Li⁺ at 30 °C, demonstrating it can be applied to lithium ion batteries.

4. Conclusion

In this study, we synthesized a series of ionic liquid block copolymers via ring-opening metathesis polymerization, and the copolymers show good thermal stability and the obvious two glass transition temperatures that indicating the strong microphase separation. Especially, the 50.7 mol% PIL copolymer exhibits good lamella morphology with long-range periodic order clearly in TEM image. In this system of polyelectrolyte, the higher PIL block compositions as well as lithium salt contents are beneficial for ionic conductivity. The polyelectrolyte with 50.7 mol% PIL compositions and 20 % LiTFSI offers the best ionic conductivities with $7.44 \times 10^{-6} \text{ S cm}^{-1}$ at 30 °C and $4.68 \times 10^{-4} \text{ S cm}^{-1}$ at 100 °C, and the values are largely improved compared to other low PIL compositions block polymers. Moreover, the polyelectrolyte also exhibits good electrochemical stability and decomposes at about 4.2 V versus Li/Li⁺. Considering that the good corresponding properties of the block copolymers, such as stability and ionic conductivity, they will be one of the potential

candidate materials for lithium ion battery.

Acknowledgement

This work is supported by the National Natural Science Foundation of China (51463014 and 21164006).

References

- 1 C.F. Yuan, J. Li, P.F. Han, Y.Q. Lai, Z.A. Zhang and J. Liu, *J. Power Sources*, 2013, **240**, 653-658.
- 2 Y. Wang, B. Li, J.Y. Ji and W.H. Zhong, *J. Power Sources*, 2014, **247**, 452-459.
- 3 Q.W. Lu, J.H. Fang, J. Yang, G.W. Yan, S.S. Liu and J.L. Wang, *J Membrane Sci.*, 2013, **425**, 105-112.
- 4 X. Zuo, X.M. Liu, F. Cai, H. Yang, X.D. Shen and G. Liu, *J. Power Sources*, 2013, **239**, 111-121.
- 5 D.F. Miranda, C. Versek, M.T. Tuominen, T.P. Russell and J.J. Watkins, *Macromolecules*, 2013, **46**, 9313-9323.
- 6 J.Y. Yuan and M. Antonietti, *Polymer*, 2011, **52**, 1469-1482.
- 7 J. M. Lu, F. Yan and J. Texter, *Prog. Polym. Sci.*, 2009, **34**, 431-448.
- 8 M. Armand, F. Endres, D.R. MacFarlane, H. Ohno and B. Scrosati, *Nat. Mater.*, 2009, **8**, 621-629.
- 9 M. T. Li, B. L. Yang, L. Wang, Y. Zhang, Z. Zhang, S. H. Fang and Z. X. Zhang, *J. Membr. Sci.*, 2013, **447**, 222-227.
- 10 M. T. Li, L. Wang, B. L. Yang, T. T. Du and Y. Zhang, *Electrochim. Acta*, 2014,

- 123**, 296-302.
- 11 Y. S. Ye, J. H. Choi, K. I. Winey and Y. A. Elabd, *Macromolecules*, 2012, **45**, 7027-7035.
- 12 J. H. Choi, Y. S. Ye, Y. A. Elabd and K. I. Winey, *Macromolecule*, 2013, **46**, 5290-5300.
- 13 K. Yin, Z. X. Zhang, L. Yang and S. I. Hirano, *J. Power Sources*, 2014, **258**, 150-154.
- 14 M. D. Green, J. H. Choi, K. I. Winey and T. E. Long, *Macromolecules*, 2012, **45**, 4749-4757.
- 15 Y. Schneider, M. A. Modestino, B. L. McCulloch, M. L. Hoarfrost, R. W. Hess and R. A. Segalman, *Macromolecules*, 2013, **46**, 1543-1548.
- 16 M. Lee, U. H. Choi, R. H. Colby and H. W. Gibson, *Chem. Mater.*, 2010, **22**, 5814-5822.
- 17 M. Döbbelin, I. Azcune, M. Bedu, A. R. Luzuriaga, A. Genua, V. Jovanovski, G. Cabañero and I. Odriozola, *Chem. Mater.*, 2012, **24**, 1583-1590.
- 18 M. T. Li, L. Yang, S. H. Fang, S. M. Dong, S. Hirano and K. Tachibana, *J. Power Sources*, 2011, **196**, 8662-8668.
- 19 M. T. Li, L. Yang, S. H. Fang, S. M. Dong, S. Hirano and K. Tachibana, *Polym Int*, 2012, **61**, 259-264.
- 20 S. Biswas, K. D. Belfield, R. K. Das, S. Ghosh and A. F. Hebard, *Chem. Mater.*, 2009, **21**, 5644-5653.
- 21 H. R. Allcock, J. D. Bender, R. V. Morford and E B. Berda. *Macromolecules*, 2003,

- 36**, 3563-3569.
- 22 M. R. Xie, J. Y. Dang, J. X. Shi, H. J. Han, C. M. Song, W. Huang and Y. Q. Zhang, *Acta Chim. Sinica*, 2009, **67**, 869
- 23 R. L. Weber, Y. S. Ye, A. L. Schmitt, S. M. Banik, Y. A. Elabd and M. K. Mahanthappa, *Macromolecules*, 2011, **44**, 5727-5735.
- 24 E. F. Wiesenauer, J. P. Edwards, V. F. Scalfani, T. S. Bailey and D. L. Gin, *Macromolecules*, 2011, **44**, 5075-5078.
- 25 H. Chen, J. H. Choi, D. S. Cruz, K. I. Winey and Y. A. Elabd, *Macromolecules*, 2009, **42**, 4809-4816.
- 26 W. S. Chi, S. U. Hong, B. Jung, S. W. Kang, Y. S. Kang and J. H. Kim, *J Membrane Sci.*, 2013, **443**, 54-61.
- 27 N. Leventis, C. S. Leventis, D. P. Mohite, Z. J. Larimore, J. T. Mang, G. Churu and H. B. Lu. *Chem. Mater.*, 2011, **23**, 2250-2261.
- 28 S. Ahn, P. Deshmukh and R. M. Kasi, *Macromolecules*, 2010, **43**, 7330-7340.
- 29 S.H. Yeon, S.H. Ahn, J.H. Kim, K.B. Lee, Y. Jeong and S.U. Hong, *Polym. Adv. Technol.*, 2012, **23**, 516-521.
- 30 M. A. Ratner, J. R. MacCallum and C. A. Vincent, *Inc.: New York*, 1987, **173**.
- 31 M. Armand, *Solid State Ionics*, 1983, **9-10**, 745-754.
- 32 Y. F. Zhang, C. A. Lim, W. W. Cai, R. Rohan, G. d. Xu, Y. B. Sun and H. S. Cheng, *RSC Adv.*, 2014, **4**, 43857-43864.
- 33 I. Stepniak, E Andrzejewska, A Dembna and M Galinski, *Electrochim. Acta*, 2014, **121**, 27-33.

- 34 F. Cai, X. Zuo, X. M. Liu, L. Wang, W. Zhai and H. Yang, *Electrochim. Acta*, 2013, **106**, 209- 214.
- 35 J. R. Nykaza, Y. S. Ye and Y. A. Elabd, *Polymer*, 2014, **55**, 3360-3369.
- 36 W. Xiao, C. Miao, X.Q. Yin, Y.C. Zheng, M.L. Tian, H. Li and P. Mei. *J. Power Sources*, 2014, **252**, 14-20.

Table 1 Compositions and thickness of polyelectrolyte membranes.

Sample(PIL mole percentage)	LiTFSI(%) ^a / thickness (μm) ^b			
21.3 mol%	5/150	-	-	-
24.2 mol%	5/148	-	-	-
31.0 mol%	5/150	10/146	15/152	20/150
38.7 mol%	5/148	10/152	15/150	20/148
50.7 mol%	5/150	10/154	15/150	20/148

^a The Weight ratio of LiTFSI/copolymer (wt.%).

^b The thickness of electrolyte membranes.

- The electrolyte membranes are not prepared due to the ionic conductivity is very low with the 5% LiTFSI content.

Table 2 Molecular Characteristics of copolymers.

PIL Diblock copolymers ¹	Feed ratio of PIL mol%	Actual ratio of PIL mol%	Mn(g mol ⁻¹)	PDI	T _d (°C)	T _{g1} (°C)	T _{g2} (°C)
PMN	0	0	27874	1.04	281	-	41.39
21.3 mol%	20	21.3	33229	1.06	385	-1.33	48.98
24.2 mol%	25	24.2	33252	1.93	391	-3.30	48.98
31.0 mol%	33	31.0	33502	1.04	394	-4.30	51.24
38.7 mol%	40	38.7	34637	1.17	327	-4.98	51.24
50.7 mol%	50	50.7	37674	2.10	400	-4.98	51.24

¹Numbers correspond to PIL mol % that is calculated by ¹H NMR spectroscopy.

Table 3 Ionic Conductivity of polyelectrolyte with different lithium salt contents

Copolymer electrolytes	Conductivity (×10 ⁻⁶ S cm ⁻¹)							
	LiTFSI(5%)		LiTFSI(10%)		LiTFSI(15%)		LiTFSI(20%)	
Temperature/ °C	30	100	30	100	30	100	30	100
50.7mol%	1.58	156	2.02	201	4.27	289	7.44	468
38.7 mol%	1.09	154	1.55	184	3.97	239	7.18	272
31.0 mol%	0.78	94	1.33	137	2.51	169	3.97	203

Captions for Scheme and Figures:

Scheme 1. Synthesis routes for monomers and copolymers.

Fig. 1. The photograph of electrolyte membrane.

Fig. 2. ^1H NMR of NIm-TFSI (a) and copolymers (b).

Fig. 3. TGA thermogram of PIL diblock copolymers.

Fig. 4. DSC thermograms of copolymers (a) and polyelectrolyte of 50.7 mol% PIL with different lithium salt contents (b).

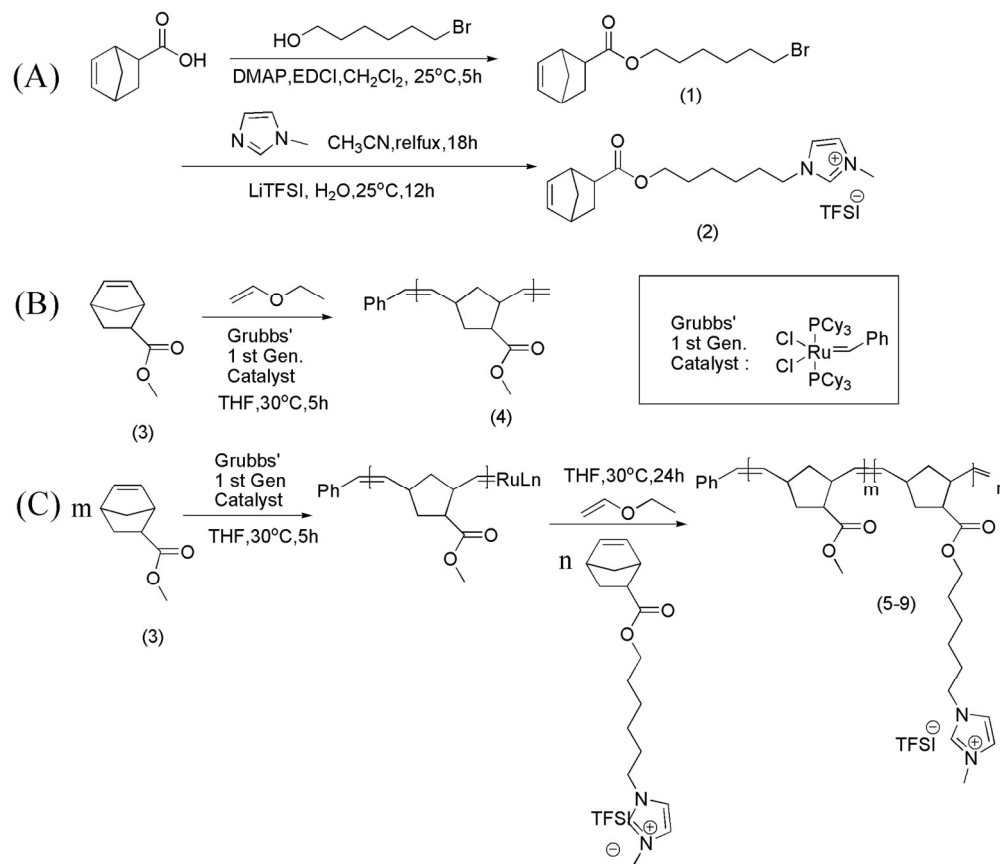
Fig. 5. XRD patterns of copolymers.

Fig. 6. TEM of copolymers: a: 21.3 mol% PIL; b: 31.0 mol% PIL; c: 50.7 mol% PIL.

Fig. 7. Temperature dependence of ionic conductivity of polyelectrolyte with 5% LiTFSI.

Fig. 8. Temperature dependence of ionic conductivity of polyelectrolyte of 50.7 mol% PIL with various LiTFSI components.

Fig. 9. Linear sweep voltammetry curves of the cells prepared for electrolytes with 20%LiTFSI. (1mV s^{-1} , SS: Stainless Steel)



Scheme 1. Synthesis routes for monomers and copolymers
161x139mm (300 x 300 DPI)



Fig. 1. The photograph of electrolyte membrane.
29x31mm (300 x 300 DPI)

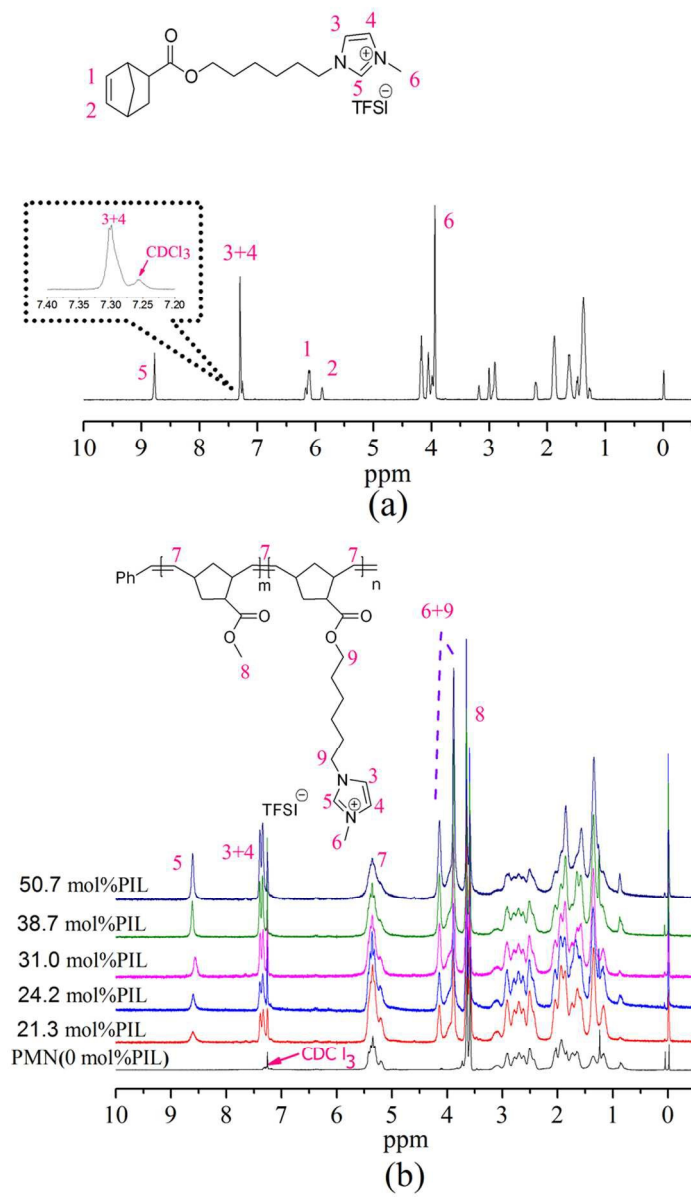


Fig. 2. ^1H NMR of NIm-TFSI (a) and copolymers (b).
254x432mm (300 x 300 DPI)

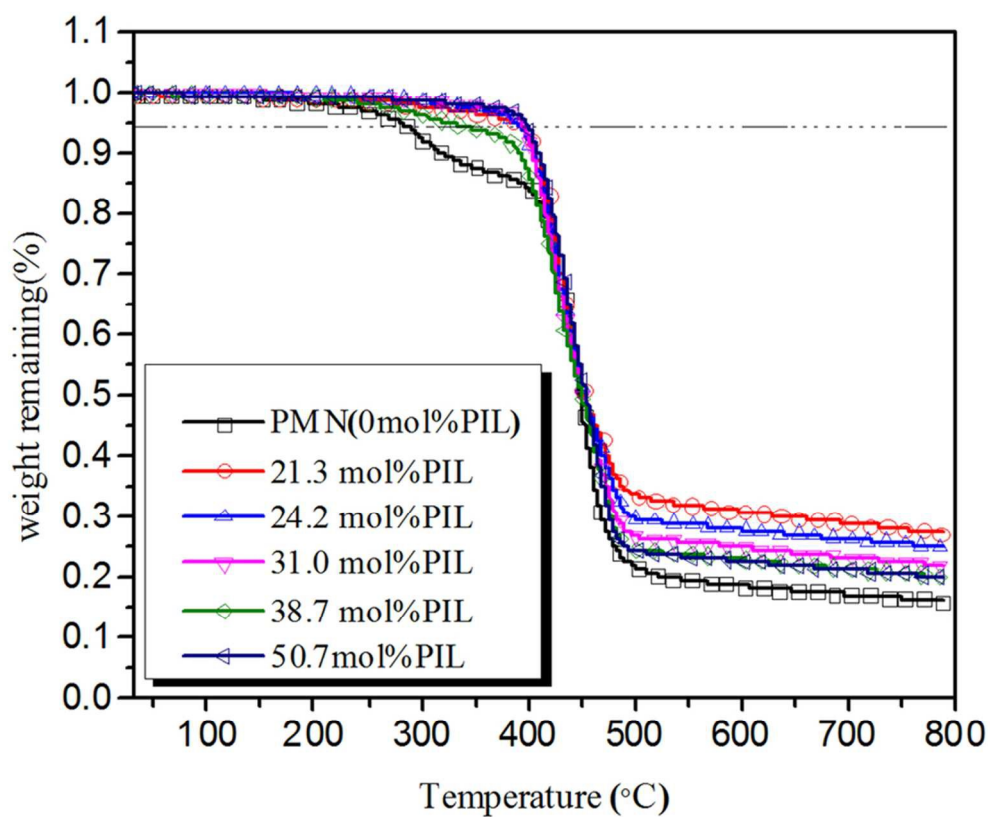


Fig. 3. TGA thermogram of PIL diblock copolymers
77x64mm (300 x 300 DPI)

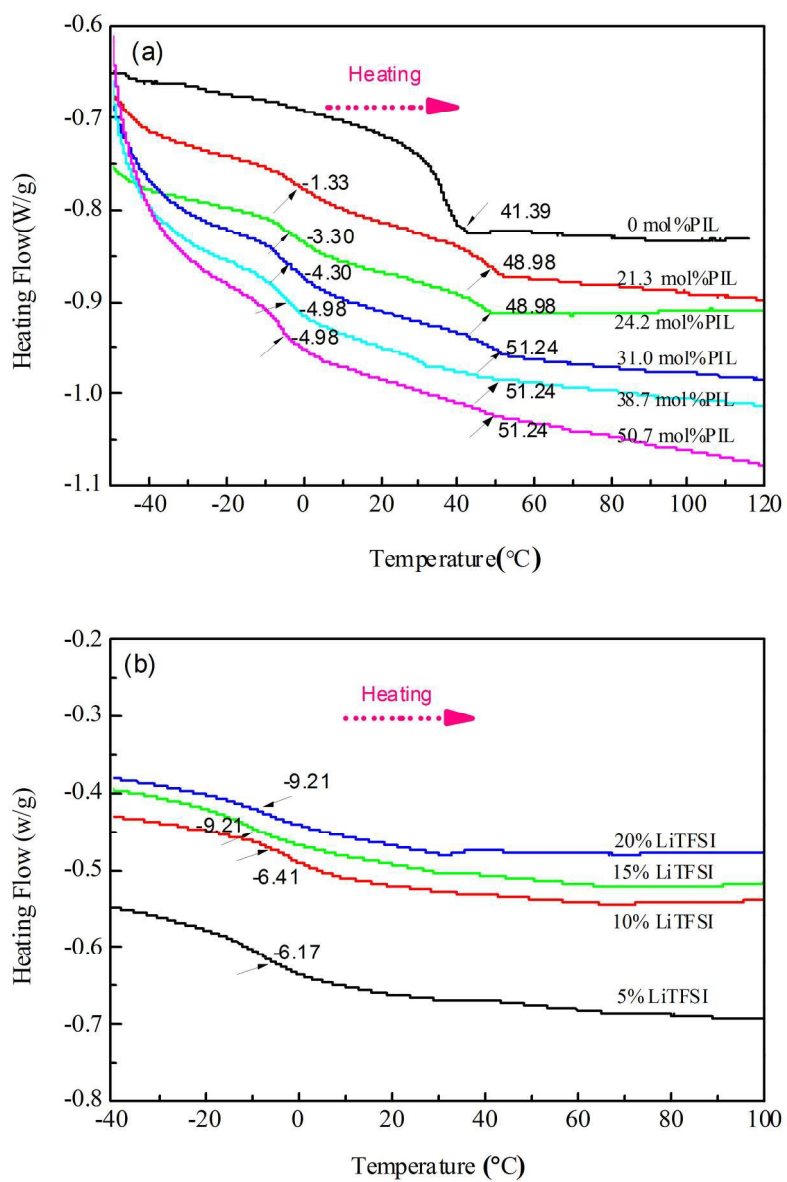


Fig. 4. DSC thermograms of copolymers (a) and polyelectrolyte of 50.7 mol% PIL with different lithium salt contents (b).

163x242mm (300 x 300 DPI)

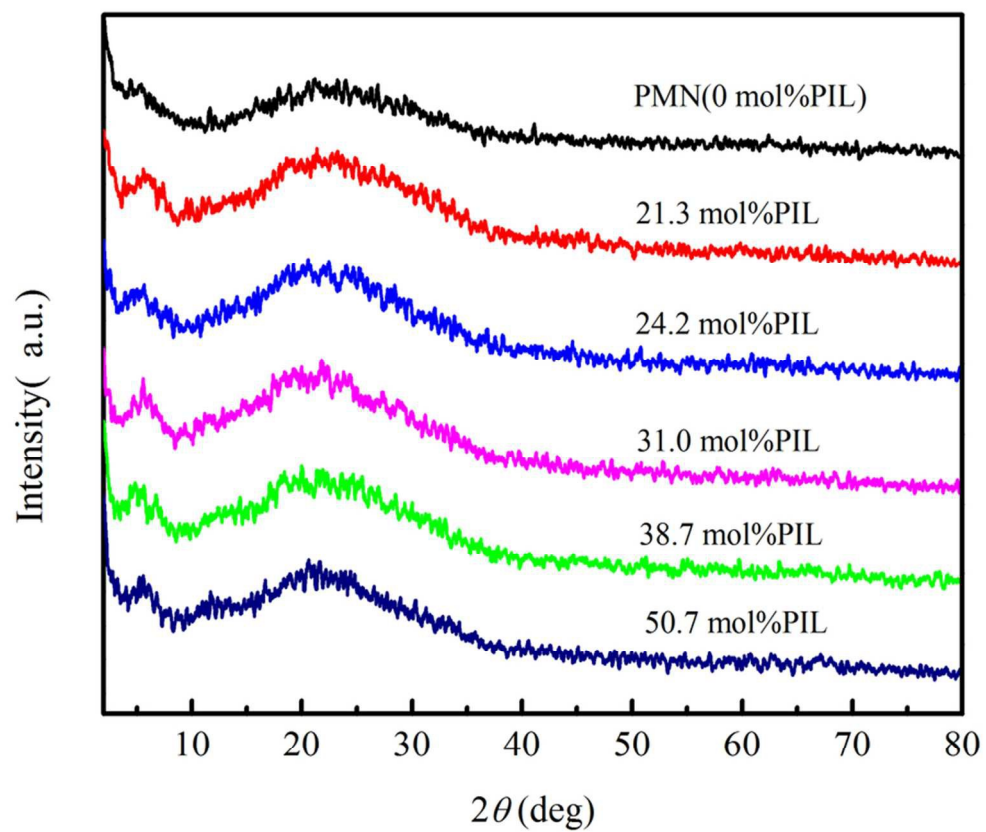


Fig. 5. XRD patterns of copolymers.
77x67mm (300 x 300 DPI)

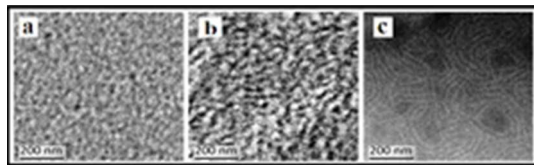


Fig. 6. TEM of copolymers: a: 21.3 mol% PIL; b: 31.0 mol% PIL; c: 50.7 mol% PIL.
22x6mm (300 x 300 DPI)

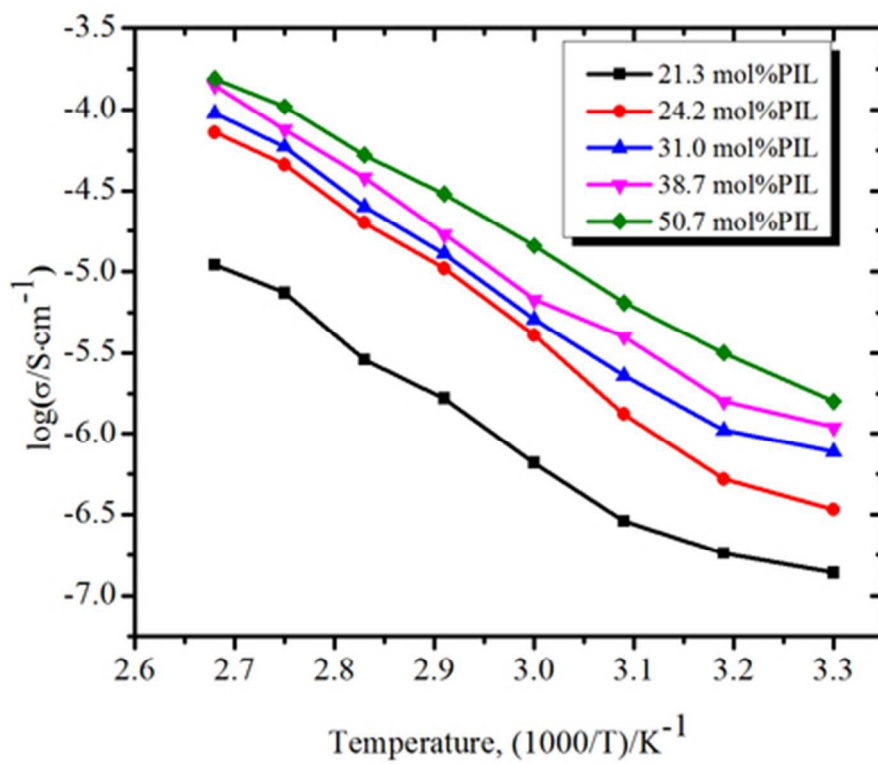


Fig. 7. Temperature dependence of ionic conductivity of polyelectrolyte with 5% LiTFSI.
38x32mm (300 x 300 DPI)

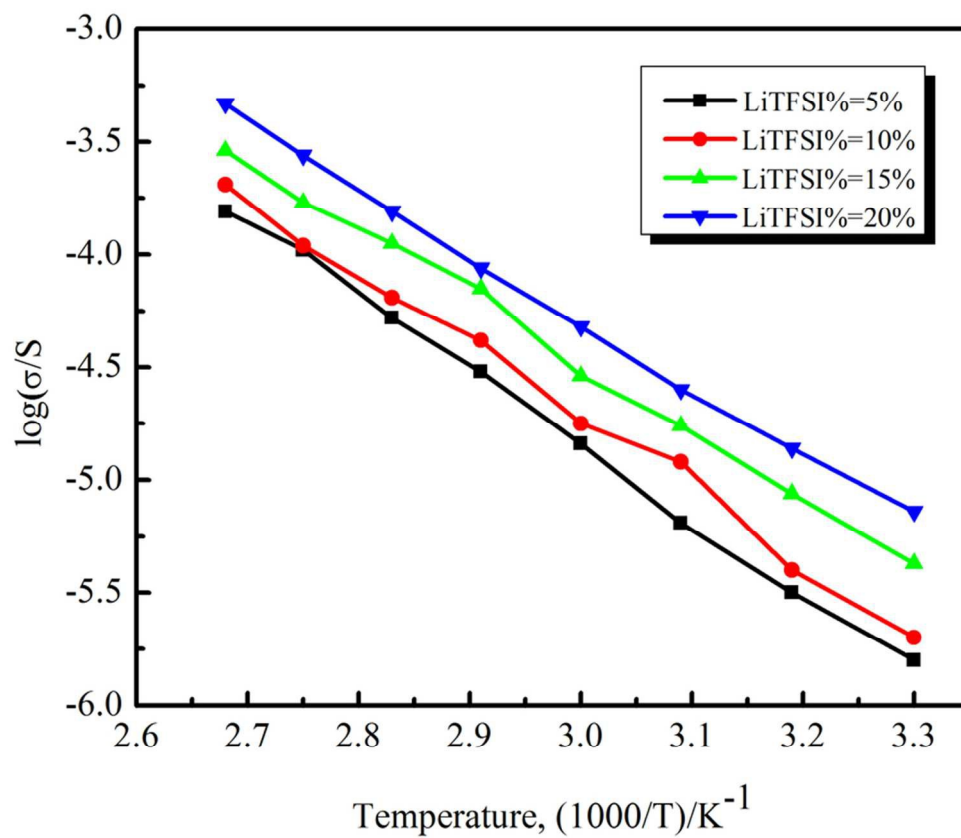


Fig. 8. Temperature dependence of ionic conductivity of polyelectrolyte of 50.7 mol% PIL with various LiTFSI components.
78x67mm (300 x 300 DPI)

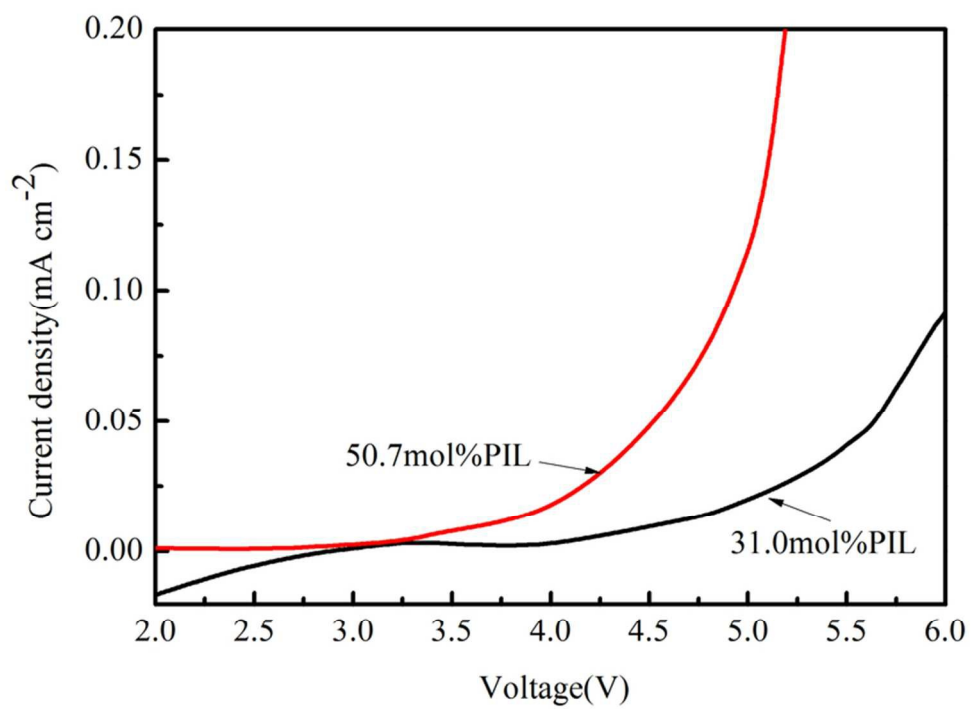


Fig. 9. Linear sweep voltammetry curves of the cells prepared for electrolytes with 20%LiTFSI (1mV s⁻¹, SS: Stainless Steel).
73x53mm (300 x 300 DPI)

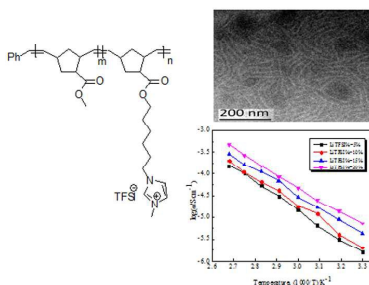
Table of content

Preparation of ROMP-type Imidazolium-Functionalized Norbornene Ionic Liquid Block Copolymer and Electrochemical Property for Lithium-ion Battery

Polyelectrolyte Membranes

Juan Wang¹, Xiaohui He^{1,2*}, Hongyu Zhu¹, and Defu Chen³

Solid polymer electrolytes with high ionic conductivity have been prepared based on imidazolium-functionalized norbornene ionic liquid block copolymer.



* Correspondence to: Xiaohui He, School of Materials Science and Engineering, Nanchang University, Nanchang 330031, China. Email: hexiaohui@ncu.edu.cn (X. He)